UC Santa Barbara
UC Santa Barbara Previously Published Works

Title

Evaluating Drought Impact on Postfire Recovery of Chaparral Across Southern California

Permalink

https://escholarship.org/uc/item/2qx3w9xz

Journal

Ecosystems, 24(4)

ISSN

1432-9840

Authors

Storey, Emanuel A
Stow, Douglas A
Roberts, Dar A
et al.

Publication Date

2021-06-01

DOI

10.1007/s10021-020-00551-2

Peer reviewed

Evaluating Drought Impact on Postfire Recovery of Chaparral Across Southern California

Emanuel A Storey[1], **Douglas A. Stow**[1], **Dar A. Roberts**[2], **John F. O'Leary**[1], **Frank W. Davis**[3]

[1]Department of Geography, San Diego State University, 5500 Campanile Drive, San Diego, California 92182, USA;

[2]Department of Geography, University of California-Santa Barbara, 3611 Ellison Hall, Santa Barbara, California 93106, USA;

[3]Bren School of Environmental Science and Management, University of California-Santa Barbara, 2400 Bren Hall, Santa Barbara, California 93106, USA

Abstract

Chaparral shrubs in southern California may be vulnerable to frequent fire and severe drought. Drought may diminish postfire recovery or worsen impact of short-interval fires. Field-based studies have not shown the extent and magnitude of drought effects on recovery, which may vary among chaparral types and climatic zones. We tracked regional patterns of shrub cover based on June-solstice Landsat Normalized Difference Vegetation Index series, compared between the periods 1984–1989 and 2014–2018. High spatial resolution ortho-imagery was used to map shrub cover in distributed sample plots, to empirically constrain the Landsat-based estimates of mature-stage lateral canopy recovery. We evaluated precipitation, climatic water deficit (CWD), and Palmer Drought Severity Index in summer and wet seasons preceding and following fire, as regional predictors of recovery in 982 locations between the Pacific Coast and inland deserts. Wet-season CWD was the strongest drought-metric predictor of recovery, contributing 34–43 % of explanatory power in multivariate regressions (R^2 =0.16–0.42). Limited recovery linked to drought was most prevalent in transmontane chamise chaparral; impacts were minor in montane areas, and in mixed and montane chaparral types. Elevation was correlated negatively to recovery of transmontane chamise; this may imply acute drought sensitivity in resprouts which predominate seedlings at higher elevations. Landsat Visible Atmospherically Resistant Index (sensitive to live-fuel moisture) was evaluated as a landscape-scale predictor of recovery and explained the greatest amount of variance in a multivariate regression (R^2 = 0.53). We find that drought severity was more closely related to recovery differences among twice-burned sites than was fire-return interval. Summarily, drought has a major role in long-term shrub cover reduction within xeric

chaparral ecotones bounding the Mojave Desert and Colorado Desert, likely in tandem with other global change stressors.

Keywords

Vegetation change; Fire recovery; Time series analysis; Drought impact; Aridification; Ecological management

Introduction

The persistence and health of native plant communities are global conservation priorities. Vegetation modulates water, energy, nutrient, and carbon fluxes in the Earth system, while supporting critical ecosystem processes (Costanza and others 1997; Baldocchi and others 2001). Human-caused land cover transformation, disturbance, and climatic change have caused widespread loss, fragmentation, and degradation of native vegetation (Vitousek and others 1997). Landscape and global change ecologies underscore the importance of system feedbacks, thresholds, and compound impacts stemming from multiple stressors (Turner 2010). Abnormal regimes of drought and fire may conjointly alter successional processes which determine composition, structure, and ecological functionality of plant communities (Batllori and others 2019). Meteorological phenomena associated with drought and stemming from climatic change are perhaps the most complex and least understood drivers of ecological change.

Unusually severe and protracted drought episodes have impacted the southwestern USA in recent decades (Williams and others 2013). In some areas, these droughts have increased the frequency and severity of fire due to prolonged warm seasons, elevated vapor pressure deficits, and excessive dry fuel production (Westerling and others 2006; Williams and others 2013; Seager and others 2015). This study focuses on the chaparral shrublands of southern California, where droughts occurred in the recent periods 1987–1990, 1996–1997, 2000–2002, 2007–2008, and 2012–2016 (MacDonald and others 2007; Griffin and Anchukaitis 2014; Mao and others 2015). The severity of the most recent (2012–2016) drought was unprecedented in California during the past 1200 years, and climate models predict increase of 'mega-drought' episodes during the twenty-first century (Griffin and Anchukaitis 2014; Yoon and others 2015). The evergreen sclerophyllous woody shrubs which comprise chaparral are adapted to seasonal (June-October) dry periods, and their persistence under highly variable inter-annual precipitation linked to El Niño-Southern Oscillation (ENSO) implies some level of drought tolerance (Kolb and Davis 1994; Cayan and others 1999). Episodes of water deficit that exceed thresholds of biological tolerance and adversely modify natural systems are described as 'ecological drought' (Crausbay and others 2017).

Thresholds and long-term consequences of ecological drought in chaparral are challenging to identify, especially where compounded by fire disturbance (Batllori and others 2019). Fire activity in southern California is known to vary according to precipitation receipt and wind activity (Moritz and others 2010) and may therefore shift in response to future climatic change. Fires that recur at brief intervals (< 5–15 years) may diminish chaparral recovery by reducing seedbank production (Lippitt and others 2013; Syphard and others 2019b). In this

study, we evaluate the effects of drought as well as fire-return interval on levels of mature-stage (10 years) postfire recovery in chaparral.

Early research showed that shallow- and deep-rooted chaparral species can fail to develop new growth in drought years (Harvey and Mooney 1964). More severe impacts range from branch dieback to widespread mortality (Davis and others 2002; Venturas and others 2016). Drought impacts are linked to hydraulic failure of xylem tissue under evaporative stress, and to carbon storage deficit under impeded photosynthetic conditions (Oechel and Lawrence 1981; Diffenbaugh and others 2015). Multi-annual drought leads to gradual biochemical and soil-moisture deficits, whereas seasonal drought conditions determine thermal extrema and evaporative potentials (compare McDowell and others 2008; Serra-Diaz and others 2016). The timing of drought-induced die-offs suggests that chaparral is impacted more by drought intensity than duration, though both are potentially important (Pausas and others 2016; Venturas and others 2016).

Drought may impact chaparral differentially per functional types: *obligate seeders* depend on fire-cued seed banks for regeneration, are generally shallowly rooted, and typically occur in xeric sites; *obligate resprouters* regenerate vegetatively (typically from root-crowns), are deeply rooted, and predominate mesic sites; *facultative seeders* exhibit resprouting and seeding capacities, and can span wide climatic ranges (see Jacobsen and Pratt 2018 for species information). Chaparral species with relatively shallow root systems (including *Adenostoma fasciculatum, Arctostaphylos*, and *Ceanothus* spp.) exhibit prevalent mortality in drought (Paddock and others 2013; Venturas and others 2016).

When coupled with fire disturbance, drought can also result in mortality of deeply rooted resprouters associated with mesic sites (Pratt and others 2014). Both seedlings and resprouts of chaparral may continue to be sensitive to drought in early years of postfire recovery (Parsons and others 1981; Frazer and Davis 1988; Pratt and others 2014). Drought exposes fragile chaparral seedlings to thermal and evaporative stresses (Mills 1983; Frazer and Davis 1988). Resprouting shrubs are most vulnerable to dehydration during regrowth after fire (Jacobsen and others 2016; Pausas and others 2016). Carbohydrate deficit in resprouters can increase susceptibility to pathogens and diminish regrowth vigor (Radosevich and Conard 1980; Jacobsen and Pratt 2018).

Surprisingly, little research exists on the topic of drought as a control on postfire chaparral recovery (Jacobsen and Pratt 2018). A temporal analysis of drought impact on recovering chaparral may explain variations that are unresolved by fire history and other spatial predictor variables. Repeated burning at intervals of less than 10 years has been shown through field-based studies to diminish chaparral recovery and to promote invasion by exotic plants (Zedler and others 1983; Jacobsen and others 2004; Keeley and Brennan 2012). However, field-based studies may not have captured processes that operate across broader spatial domains (Meng and others 2014). Our review of subregional investigations suggests that fire-return interval explains recovery variation more directly in some areas than others (*cp*. Lippitt and others 2013; Meng and others 2014; Syphard and others 2019a, b). Chaparral areas that receive high mean annual precipitation tend to exhibit high shrub cover and low exotic plant cover, attributed to high fire severity covariate with biomass (Smith and

others 2019). Previous large-scale studies of chaparral recovery have not analyzed the influence of drought in a temporal manner, in conjunction with fire-return interval. Estimation of vegetation change in a wide range of sites representing varied disturbance histories is required for such an analysis (compare Lippitt and others 2013).

Multi-spectral image data from satellite and aerial systems are useful to characterize large-scale patterns of recovery after fire in Mediterranean-type shrublands (Viedma and others 1997; Shoshany 2000; Díaz-Delgado and Pons 2001; Díaz-Delgado and others 2002; Riaño and others 2002; Wittenberg and others 2007; Minchella and others 2009; Gouveia and others 2010; Solans Vila and Barbosa 2010; Vicente-Serrano and others 2011; Lanorte and others 2014; Meng and others 2014; Petropoulos and others 2014; Fernandez-Manso and others 2016). Archived imagery from Landsat (4, 5, 7, and 8) is particularly useful to track inter-annual change in heterogeneous chaparral, owing to 30-m spatial resolution, 16-day revisit time, and a record spanning from 1984 to present for southern California. Signals of vegetation change are enhanced by Landsat surface reflectance products, which reduce atmospheric and solar irradiance artifacts (Masek and others 2006). Multi-annual trends of Landsat-derived Normalized Difference Vegetation Index (NDVI) capture trajectories of change in fractional shrub cover (FSC) associated with postfire recovery (Hope and others 2007; Röder and others 2008). High spatial resolution aerial imagery supports empirical calibration of Landsat NDVI data to units of FSC for the purpose of ecological change analysis (Fraser and others 2011).

Objectives and Scope

The major objective of this study is to evaluate impacts of drought on postfire recovery of chaparral across the southern California coastal eco-region (116° 25′–119° 25′ W; 32° 30′ –34° 40′ N). We leveraged the regional coverage and multi-decadal time span of Landsat image series, in order to track recovery in the greatest possible number of sites that burned since the earliest-available image from 1984. Fires within this study period (1984–2018) correspond to unique drought and non-drought episodes, and a variety of fire-return intervals in areas that burned twice. The study areas are in chamise, mixed, and montane chaparral community types and exhibit varied aridity, terrain, and recovery patterns. We conducted spatial-temporal evaluations of drought effects on recovery, based on fire history, terrain, mean climate, and three different metrics of drought intensity in seasons preceding and following the fire events. This study addresses three major research objectives according to following questions:

1. Does postfire recovery at mature stage vary significantly due to drought in summer and wet seasons preceding or following singular fire events?

2. Is drought a significant regional predictor of postfire recovery among sites that burned twice, at intervals ranging from 1 to 23 years?

3. Which geospatial terrain, vegetation, soil, and aridity variables best predict landscape-scale variation in drought-fire impact?

Methods

Overview

Figure 1 illustrates the methodological framework of this study. Historical fire perimeters obtained from California Fire Resource and Protection (FRAP) were overlaid upon maps of plant community type, in order to select potential study areas consisting of chaparral that burned after the first year of available Landsat data (1984). Refined maps of burned area in the study region were then constructed using Landsat imagery in order to the reliability of sample locations. Detailed maps of shrub cover derived from aerial ortho-imagery were used to generate linear regressions between FSC and Landsat NDVI in widely distributed sample plots. Landsat NDVI values thereby related to FSC were used to derive spatially extensive prefire (1984–1989) and postfire (2014–2018) shrub cover estimates, which were compared arithmetically in order to map variations in recovery at mature (10–33 years) postfire stages. Postfire recovery variations were evaluated based on random point samples stratified within three climatic zones, using linear regressions involving multiple spatial and temporal variables. As a temporal analysis, drought conditions were indexed according to wet and summer seasons of the 2 years preceding and 3 years following each fire event. A group of neighboring sites that exhibited low recovery due to drought were used for the spatial component of this study, in which we evaluated landscape-scale variations in terrain and aridity as modulators of drought impact. The results were synthesized to evaluate the relative importance of drought versus fire-return interval in postfire chaparral recovery across southern California.

Landsat Imagery

The Landsat images utilized in this study were processed to directional surface reflectance by the Land Surface Reflectance Climate Data Record (LSRCDR) of the United States Geologic Survey (USGS) (espa.cr.usgs.gov) (Masek and others 2006; Vermote and others 2016). These Landsat images cover the chaparral areas of southern California and coincide with Worldwide Reference System (WRS) path-rows 40–36, 40–37, 41–36, and 42–36. Shrub cover dynamics were evaluated using series of annual Landsat observations between 10 June and 14 July, a period of high solar illumination and senescence in under-storey herbs. These near-anniversary image series covered two 5-year periods which we defined as *prefire* (1984–1989) and *postfire* (2014–2018). A separate collection of Landsat images from various years and seasons were used to map burned areas. All Landsat images were masked for clouds and cloud-shadows based on Fmask quality-assurance maps provided by LSRCDR (Zhu and Woodcock 2012). Landsat pixels flagged by Fmask were supplanted with cloud-free pixels from images of proximal acquisition dates.

Fire History, Site Selection, and Stratification

Study areas were selected throughout southern California based on shrub community type and fire history criteria. Community types included *montane, mixed*, and *chamise* chaparral. Chamise is dominated by *Adenostoma fasciculatum* (in excess of 60% relative cover); mixed chaparral is co-dominated by *A. fasciculatum, Ceanothus* spp., *Arctostaphylos* spp., and *Quercus berberidifolia*; montane chaparral is composed largely of *Arctostaphylos patula, C. cordulatus, C. integerrimus, C. velutinus, Cercocarpus ledifolius*, and *Chrysolepis*

sempervirens. These community types are most prevalent in southern California according to CALYEG maps developed in 1980, prior to the period of our study (Matyas and Parker 1980; fs.usda.gov). More recent FVEG maps show the same chaparral community types as more extensive in some areas (fs.usda.gov). Therefore, we utilized a spatial union of the FVEG and CALVEG chaparral classes, affording priority to CALVEG maps in cases of conflict.

All areas that burned more recently than 1974—and that coincide with the chaparral community types of interest—were identified using fire perimeter data of FRAP (calfire.gov). Areas that burned in the periods 1975–1984 and 2009–2018 were then excluded from our study (with exceptions noted below) because such areas may contain shrubs that were immature during prefire (1984–1989) or postfire (2014–2018) assessment periods. This criterion for excluding immature sites is based on findings that postfire recovery of chaparral is a 10-year process (McMichael and others 2004; Hope and others 2007; Storey and others 2016). We included matured chaparral areas that burned in the period 1985–2008 as prospective study areas. We selected the maximum possible extent of study area that burned in this 24-year period.

Fire history since 1984 in the prospective study areas was reconstructed based on Landsat Normalized Bum Ratio (NBR) data (Key and Benson 1999), for the reason that FRAP fire perimeters are shown to contain inaccuracies (Syphard and Keeley 2017). We derived *prefire-to-posifire* NBR difference (dNBR) and relative-difference (RdNBR) bum severity indices, using formulas given by Miller and Thode (2007). These burn severity indices were used conjointly to identify burned areas, which were then classified using value-exceedance criteria that we identified through iterative pixel queries and inspection of binary map results. In this procedure, we classified a total of 155 Landsat images, many of which recorded several fire scars.

We excluded human-built features from the study areas by manual delineation based on 0.6-m spatial resolution, color-infrared ortho-imagery captured in 2016 by the National Agriculture Imagery Program (earthexplorer.usgs.gov). After masking out built features and immature chaparral sites, we obtained a set of 240 contiguous areas (hereafter: *stands*) which are internally uniform with respect to shrub community type and fire history during the study period. These stands range from 1 to 557 km^2 (19 ± 44 km^2, $\bar{x}$ ± SD). Approximately 92% of the collective study area (173 stands) burned once, whereas eight percent of it (67 stands) burned twice at intervals of 1–23 years (Figure 2).

Stands were organized into three custom-defined climatic zones based on geographic position and mean annual precipitation (prism.oregonstate.edu). We defined the *montane* zone as high-elevation areas that receive at least 500 mm y^{-1} of precipitation (Figure 2). The *cismontane* zone receives less than 500 mm yr^{-1} of precipitation and spans from the Pacific Coast to the montane zone. The *transmontane* zone also receives less than 500 mm y^{-1} in precipitation, but is located on the leeward (rain shadow) sides of the Transverse and Peninsular Ranges, and includes the xeric chaparral ecotone which intergrades into desert vegetation.

Estimation of Vegetation Change

We evaluated recovery on the basis of change in shrub cover between the prefire period and the end of the postfire period, which allowed 10 or more years of recovery in the study areas. Estimates of recovery were based on temporal trajectories of Landsat NDVI, as illustrated in Figure 3. Trajectories derived in five-year periods are less sensitive to the effects of variable precipitation on annual leaf production than are single-year values (Riaño and others 2002). Postfire trajectories (2014–2018) were characterized by linear best-fit functions, to capture potential increase of shrub cover at sites that burned in 2004–2008. Postfire NDVI values were extracted from termini of the best-fit trajectories, which coincide with 21 June 2018. Prefire values were based on mean NDVI from the prefire period (1984–1989) in which vegetation abundance was assumed to be stable in the study areas. Several areas of interest had burned after 2016, or in the early years of the prefire period. Accordingly, we excluded data points of years following these fire events from the NDVI trajectories. For areas that burned in 1985, 1986, 1987, or 1988, we included only the NDVI values that precede these years into the prefire mean calculations.

Detailed maps of shrub cover were generated from the 2016 ortho-imagery in order to derive estimates of FSC from Landsat NDVI. Chaparral within the study region was delineated into 49 distinct polygonal segments, defined by visual interpretation of the CALVEG maps and ortho-imagery as having internally consistent shrub community types and canopy density patterns. At least one calibration plot of 3-km × 3-km dimensions was placed in each segment. Shrub cover maps of the plots were generated using decision-tree, threshold-based classifiers which we developed using ERDAS IMAGINE® image processing software. The classifications were based on spectral image transforms including NDVI, intensity (mean of visible bands), and red-to-intensity ratio (diagnostic of exposed soils). We selected and iteratively refined thresholds based on pixel query and inspection of trial output results. This mapping approach yields 87–95% accuracy when applied to chaparral (Storey and others 2016). We present an example of the ortho-image data (Figure 4A, B) used to derive a three-class land cover map (Figure 4C).

Areal fractions of shrub cover were tabulated using 90-m × 90-m sampling grids which we imposed on the calibration plots. We aggregated by averaging the 3×3 Landsat NDVI pixel arrays within these grid elements (subplots), to reduce the spurious effects of geometric misregistration among images from the time series (compare Hope and others 2007). Thirty grid elements were sampled randomly from each plot, at 150-m minimum spacing to prevent selection of adjacent grid elements. Grid data samples were used to relate Landsat NDVI and FSC in each of the 49 segments, using slope and intercept values derived from ordinary least-squares (OLS) regressions. Coefficient of determination (R^2) values indicating goodness-of-fit in the plot-based Landsat NDVI-FSC regressions ranged from 0.56 to 0.95, with a mean value of 0.83 and standard deviation of 0.13. Arithmetic differencing of prefire versus postfire FSC produced a regional map of absolute percent change in fractional shrub cover (hereafter: *dFSC*).

Geospatial Data

Data sets described in Table 1 were used as potential explanatory variables. Previous work suggests that terrain can modulate drought impact according to sun exposure, soil properties, and moisture accumulation (Meentemeyer and Moody 2002). We evaluated seven edaphic variables from the State Soil Geographic (STATSGO) including textural, hydrologic, and thickness properties (nrcs.usda.gov). A 30-m digital elevation model (ned.usgs.gov) was used to derive topographic slope, aspect, solar irradiance from spring to autumn equinoxes, and curvature variables which are potential controls on plant establishment (Davis and Goetz 1990). As riparian chaparral may be affected differently by drought (Coates and others 2015), we inferred riparian zones based on 30-m proximity to hydrologic channels (data.cnra.ca.gov).

Mean annual precipitation, temperature, and vapor pressure deficit were evaluated based on Parameter-elevation Regressions on Independent Slopes Model (PRISM) data gridded at 800-m resolution (Daly and others 1994; prism.oregonstate.edu). Landsat images acquired on 13 June 1986 were used to derive Visible Atmospherically Resistant Index (VARI) (Gitelson and others 2002), which is sensitive to live-fuel moisture (LFM) in chaparral (Stow and others 2005; Roberts and others 2006; Peterson and others 2008). The VARI is based on visible (red, green, and blue) spectral bands and therefore is not a direct correlate of NDVI. We based VARI on Landsat images from early June because transpiration is expected to be high at this time, while the summer 'dry-down' phase is just beginning (compare Coates and others 2015). The year 1986 was a near-average precipitation year and preceded fire in the relevant study areas. Because VARI and plant cover are potentially correlated (compare Gitelson and others 2002; Stow and others 2005), we normalized for shrub cover by calculating the ratio of VARI to prefire FSC. We used VARI as a proxy for spatial (but not temporal) variation in LFM.

Drought Metrics

Spatial-temporal drought metrics were based upon seasonal aggregates of monthly Palmer Drought Severity Index (PDSI) (Palmer 1965), monthly Climatic Water Deficit (CWD) (Stephenson 1998; Flint and others 2013), and monthly precipitation (PRCP) (Livneh and others 2013). The PRCP data gridded at 6-km resolution were provided by National Centers for Environmental Information (NCEI) (data.nodc.noaa.gov/livnehmodel). The PDSI index integrates soil properties with precipitation and temperature in order to simulate moisture anomalies associated with drought, and is closely related to potential evapotranspiration (Szép and others 2005). We obtained monthly PDSI data (1983–2011) gridded at 4-km resolution from WestWide Drought Tracker (Abatzoglou and others 2017; wrcc.dri.edu). The CWD represents the difference of potential and actual evapotranspiration, is closely related to plant-available moisture (Flint and others 2013), and may provide the most direct indication of drought stress in chaparral. The 270-m resolution monthly CWD data obtained through USGS are available from 1983 but span only to 2010 (Flint and others 2013; climate.calcommons.org). The monthly PDSI, PRCP, and CWD indices were aggregated per wet seasons (November-May), in which hydrologic pulses enter the chaparral system and regulate annual foliar production (compare Christensen and Muller 1975). Separately, we also aggregated the drought indices per summer 'dry-down' seasons (June-August) when

shrub foliage and air temperatures are high, but precipitation is minimal (compare Coates and others 2015). Absolute seasonal PRCP totals (mm) were evaluated separately from relative-percentage values, calculated with respect to 28-year means (1983–2011).

Analytical Procedures

We evaluated temporal as well as spatial components of recovery variation due to drought. The temporal component is based on the seasonal PDSI, CWD, and PRCP drought metrics. We defined S_0 as the wet or summer season during which a fire occurs, or as the first season after fire (mainly for wet-season drought metrics, in the many cases that fires occurred in autumn). Drought-metric values corresponding to S_0 are defined herein as PDSI-S_0, CWD-S_0, and PRCP-S_0. We defined seasonal time steps in relation to S_0, including one annual cycle after (S_{+1}), two cycles after (S_{+2}), one cycle prior (S_{-1}), and two cycles prior to S_0 (S_{-2}). Seasonal drought metrics were derived for prefire years to evaluate the hypothesis that antecedent drought can diminish recovery. Drought-metric seasons were associated with twice-burned stands according to the fire date of greater drought intensity, based on seasonal PDSI values. Each seasonal time step based on each drought index was evaluated as an independent variable.

Random vector points and rectangular polygon plots were used to sample the seasonal drought-metric grids, and to evaluate these as explanatory variables of recovery (dFSC) using multivariate linear regressions in IBM SPSS®. We collected five separate sample sets from the dFSC map that serve unique purposes: (1) stand-aggregate values ($n = 173$), used to evaluate frequency-probability of recovery across the study region; (2) aggregates of 30-m pixels (7×7 pixel-kernel means) distributed randomly throughout the single-burn areas at mean density of one per 10 km^2 ($n = 491$), used in regional evaluation of drought effects; (3) paired sample plots of 0.5-km $\times$ 0.5-km dimensions ($n = 416$), used to evaluate recovery in the twice-burned stands relative to nearby single-burn (control) stands, as a function fire-return interval and drought condition; (4) single-pixel samples distributed randomly across a selected set of 10 drought-impacted stands ($n = 697$, 1 per km^2 mean density), to explain landscape-scale spatial variation in drought impact; and (5) a set of 75 plots (0.5-km $\times$ 0.5-km) sampled from a set of 12 stands with highly varied recoveries. These 12 stands were on gradual terrain and close in proximity, which provided control for climatic setting.

The 416 paired-plot samples were placed in the closest possible proximity (2.2 ± 1.3 km, $\bar{x} \pm$ SD) and stratified according to terrain aspect and plant community type. This sample arrangement provided control for many spatial variables that can influence recovery (compare Meng and others 2014), although perfect control for terrain slope and variations internal to the 0.25 km^2 plots was not possible due to limited extent of potential sampling area. The 491 sample points were stratified per climatic zones (Figure 2), and we added climatic variables (mean annual precipitation and temperature) to the OLS regressions to account for climatic gradients within the zones.

Results

Regional Patterns of Recovery at the Stand-Aggregate Level

Mature-stage recovery levels varied substantially between and within the stands. Approximately 65% of the stands recovered to within 5% of mean prefire shrub cover. Declines in mean shrub cover of 10–15% were observed in about 32% of the stands, whereas only about 3% of the stands declined in shrub cover by more than 15%. The stands collectively exhibited strong recovery in most areas and moderate degradation in some areas. Total reduction of shrub cover that would be consistent with total 'type conversion' was not observed in any of the stands. Regional and within-stand spatial variations in recovery are discussed further below. Figure 5 illustrates how inter-annual trends in PRCP, CWD, and PDSI are related to area burned and mean stand recovery.

Based on the criterion of PDSI less than − 1.8 (Figure 5C) coupled with below-average wet-season precipitation (Figure 5D), the major drought periods lasting more than 1 year included 1989–1991, 1996–1997, 2000–2002, and 2007–2008. The three climatic zones exhibit unique fire chronologies and potentially different impacts of drought upon recovery. The montane zone contains the largest extent of burned study area. The most active fire years in each climatic zone were 2002, 2003, 2006, and 2007 (Figure 5A). Limited postfire recoveries are noted in cismontane sites that burned in the drought-proximal years 1990, 2004, and 2008 (Figure 5B). The montane stands exhibit moderate degradation (that is, decline in FSC of more than 5%), most notably in the non-drought years 1994 and 1995, but otherwise recovered well. The transmontane stands show the most prevalent and severe declines in FSC, in association with both drought and non-drought periods. A one-way analysis of variance (ANOVA) indicates a significant difference in recovery (dFSC) between regional groupings of stands that burned in drought versus non-drought years ($p = 0.01$; $F = 6.5$; $F_{crit} = 3.86$). This ANOVA does not address the potential effect of drought in years before or after fire, which is the focus of subsequent analysis based on seasonal drought metrics.

Objective 1: Evaluating Region Drought Impact in Single-Burned Sites

We evaluated seasonal drought metrics as recovery predictors based on the 491 random sample locations. Table 2 shows results from separate regression tests (refer to R^2 values) that we applied for each of the drought-metric types, which include five annual cycles (S_{-2}, S_{-1}, S_0, S_{+2}, and S_{+2}) of summer and wet seasons. Table 2 also shows *fractions of explained variance* attributable to the seasonal drought metrics; these were derived by summing the standardized β coefficients of the significant variables and computing their respective fractions (Table 2). Regressions based on data from each climate zone showed that wet-season PDSI was not a significant predictor of recovery, although summer PDSI was significant in several tests ($p < 0.05$) (Table 2). The absolute seasonal PRCP values (mm) were not significant, whereas relative-percentage wet-season PRCP metrics were significant for each climatic zone. The CWD metrics based on summer and wet seasons were significant for the cismontane and transmontane zones (Table 2). Mean annual precipitation and temperature were also significant predictors of recovery but exhibit variable effect sizes among the tests, and were omitted from Table 2 for brevity.

Statistical tests relating to the montane zone were less reliable than those relating to the other climatic zones, which contain substantially greater variations in recovery (Figure 5B). Only wet-season PRCP-S_{-2} and summer PDSI-S_{+2} were statistically significant for the montane zone (Table 2). Both PRCP-S_0 and CWD-S_0 were significant for the cismontane zone, which may imply drought impact was important in the first growth season after fire. However, cumulative water deficits in wet seasons preceding fire (CWD-S_{-1} and CWD-S_{-2}) exhibited the strongest R^2 with respect to recovery for the cismontane zone. For the transmontane zone, the regression model that includes CWD-S_{-1} and CWD-S_{+1} exhibited the highest R^2 value (Table 2). Summer CWD-S_{-2} and PDSI in most seasons (S_{-2}, S_{-1}, S_{+1}, and S_{+2}) were also significant for the transmontane zone, but yielded low R^2 values. Wet-season CWD exhibited the strongest overall relationship to recovery, and contributed 34–43% of the explanatory power in these multivariate tests, when β coefficient fractions were tabulated cumulatively across wet seasons.

Objective 2: Evaluating Regional Impacts of Fire-Return Interval Versus Drought

We first evaluated differences in recovery with respect to fire-return interval and number of burns, irrespective of drought. A comparison of the single- and multiple-bum plot sets implies no significant difference between their sample mean values (paired, one-tailed *t* test; $p = 0.11$; $F_{sig} = 0.15$). A subset of these data including only those plots that declined by more than 5% in FSC, exhibits a significant difference between the single- and multiple-burn samples ($p = 0.01$; $F_{sig} = 0.001$). The most useful metric of recovery in this application is the *difference in dFSC* between counterpart sample plots. This metric showed no significant association with fire-return interval ($p = 0.79$).

Drought effects were evaluated based on metric values from individual plots (*i.e.*, absolute values), and separately based on relative differences in drought-metric values between the counterpart plots. Results of statistical tests which evaluate the absolute and relative-difference drought metrics (with respect to relative-difference dFSC) are given in Table 3. Relative-difference seasonal PRCP metrics (S_{-2} and S_{+1}) were significant in explaining recovery differences among the paired plots. Absolute and relative-difference PDSI based on summer and wet seasons were also significant predictors of relative-difference dFSC, and yielded R^2 values higher than the PRCP metrics. The highest R^2 value (0.09) resulted from prefire summer CWD (S_{-2}). Fire-return interval was not a significant variable when included in the drought impact evaluations.

Objective 3: Evaluating Landscape-Scale Variations in Drought Impact

Ten stands were used to evaluate landscape-scale spatial predictors of recovery variation due to drought impact (Figure 6). These stands were selected by the following criteria: (1) the most recent fires in these stands were preceded or followed by a drought year; and (2) declines of shrub cover greater than 15% were observed in heterogeneous patterns across substantial portions of these stands (Figure 6). Most of these selected stands are in the transmontane zone (*cp*. Figures 2, 6F).

Exploratory OLS regression analysis led us to eliminate nonsignificant variables including solar irradiance, terrain (aspect, slope, and curvature), presence of riparian features, and

most of the STATSGO edaphic variables (available water capacity, thickness, organic matter, clay content, conductivity, and hydrologic group). Mean annual precipitation and vapor pressure deficit were eliminated due to collinearity with elevation.

Regression outputs based on the significant landscape variables are given in Table 4. Chaparral community type and soil permeability were positively related to recovery, with relatively small effect sizes according to β coefficient values (0.12 and 0.14, respectively). The positive β coefficient of the community type variable indicated greater recovery in montane (Stratum 3) and mixed (Stratum 2) as compared to chamise (Stratum 1) chaparral. Elevation exhibited a strong and negative relationship to recovery ($\beta = -0.35$). The normalized VARI exhibited the strongest relationship to recovery ($\beta = -0.38$). Model fit ($R^2 = 0.53$) suggests that the spatial variables in Table 4 explain about 53% of the variance in recovery within this selection of stands.

A separate group of 12 stands (also depicted in Figure 6F) was used to evaluate temporal effects of drought at a relatively localized scale. These stands burned in years (1990, 1995, 1999, 2002, 2003, or 2004) that represent periods with a variety of drought as well as non-drought conditions (Figure 5). These stands exhibited varied recovery levels but relatively uniform terrain and internal recovery patterns. The close proximity and similar elevations of these stands provided some control for mean climate and other environmental variables. Wet-season CWD was used in this analytical component owing to its high significance in other tests (Table 2). Unlike the regional analysis, the most recent fire among these stands occurred in 2004, which permitted evaluation of recovery metrics over five seasons following fire (2005–2010).

As shown in Table 5, CWD in several prefire wet seasons (S_{-3}, S_{-2}) and the first postfire wet season (S_0) were significant predictors of recovery, and represent substantial fractions of the explained variance (0.19–0.31). The strongest predictor of recovery was CWD-S_0 based on its low variable inflation and individual R^2 value of 0.13. Long-term (28-year) mean wet-season CWD also exhibited a significant, positive relation to recovery (Table 5). CWD-S_{-1} yielded a high individual R^2 value, but was insignificant in the multivariate test due to high variable inflation. Drought metrics based on CWD in seasons after S_0 were insignificant (Table 5). The significant drought variables in this analysis together explained 42% of the variation in recovery, based on this small mosaic of stands that were evidently more impacted by drought than others in the montane and cismontane zones.

Discussion

We utilized a 35-year series of multi-spectral Landsat surface reflectance images in order to characterize and explain variations in postfire recovery of southern Californian chaparral in relation to drought intensity over the period 1983–2011. The major goals of this study were: (1) to evaluate the effect of seasonal drought intensity on chaparral recovery among single-burned stands in montane, cismontane, and transmontane zones; (2) to comparatively evaluate the impacts of fire-return interval and drought; and (3) to evaluate a suite of geographic variables as potential predictors of landscape-scale recovery variation within areas impacted by drought.

The evidence of coupled drought-fire impacts produced in this study corroborates previous findings (Parsons and others 1981; Frazer and Davis 1988; Pratt and others 2014). Key insights gained from this study concern the magnitude, spatial variation, and relevant timing(s) of drought impact on chaparral recovery. Our results suggest that impacts of drought on recovery in recent decades were most severe in transmontane chaparral, associated with an ecotone which separates the regional arid (desert) and semi-arid (Mediterranean-type) eco-climatic zones. Paddock *and others* (2013) also report chaparral mortality in this ecotone due to drought, in absence of fire. We find that drought-fire impacts are most acute in higher-elevation transmontane sites composed of chamise chaparral. This result may reflect sensitivity in young *A. fasciculatum* resprouts, which predominate over seedlings at higher elevations (Keeley and Soderstrom 1986). An alternative explanation is that high-elevation congener plants are less adapted to thermal anomalies during drought (McCullough and others 2016). Drought also enhances freeze-cavitation susceptibility at high elevation due to moisture deficit (Davis and others 2007). Paradoxically, we find that recoveries are robust and drought effects were lesser in the montane climatic zone, which consists mainly of mixed and montane chaparral community types. Growth season precipitation antecedent to fire was a significant predictor of recovery within the montane zone. This finding may imply vulnerability to protracted drought, due to cumulative deficits of plant carbohydrates or deep soil moisture (compare Radosevich and Conard 1980; Oechel and Lawrence 1981). Based on a local mosaic of single-bum stands that exhibited highly variable recoveries, we find the clearest evidence of protracted drought impact ($R^2 = 0.42$) in wet seasons preceding and immediately following fire.

Climatic water deficit (CWD) is the strongest drought-metric predictor of recovery in the cismontane and transmontane zones. Remarkably, prefire CWD is negatively associated with recovery in the transmontane zone (Table 2). This anomaly could be explained by a surge in plant growth producing abundant fuel, which may increase subsequent fire severity and cause mortality of resprouters (Moreno and Oechel 1993). More indicative of drought impact, CWD, PRCP, and PDSI in seasons after fire show positive associations with transmontane recovery. It would be speculative to attribute this postfire drought sensitivity to plant functional traits, although Paddock and others (2013) report the greatest drought mortalities in seeding shrubs at a low-elevation, transmontane site within our study region. Potentially differential fire-drought responses among shrub species within sample areas represent a major uncertainty in this study.

Few studies have evaluated impacts of repeated fire in conjunction with drought (Jacobsen and Pratt 2018). Smith and others (2019) explained 8–21 % of the variation in shrub cover (a variable that is distinct from recovery) within the Simi Fire and Old Fire sites, and reported that most recent fire intervals were significantly related to shrub cover. However, Smith and others (2019) (compare Lippitt and others 2013) did not directly quantify shrub cover prior to the initial fires punctuating the return intervals, and the authors imply that precipitation represents a confounding influence due to the lower fire probability at relatively mesic sites. Similarly, Syphard and others (2019a, b) found that fire-return interval contributes to only 11–23% of the explained variation, and that micro-climatic and macro-dimatic site variables cumulatively explain a greater portion of recovery variation. Our statistical results based on 416 paired sample plots suggest that, whereas postfire recovery was significantly impacted

by drought, short-interval fire effects were nonsignificant. We attribute the discrepancy between our results and the latter studies (regarding short-interval fire effects) to differences in methodology including sampling chronology, measurement of prefire vegetation, and whether temporal drought influences were statistically accounted. We find that recovery variations resulted from intense drought soon after or before fire, culminating in a weak but significant effect ($R^2 = 0.05–0.09$; $p = 0.001–0.04$) that was more pronounced after multiple fires. In discussing postfire recovery variations generally, we acknowledge that sensitive chaparral species or areas were perhaps already impacted by drought or short-interval fire prior to the study period (compare Meng and others 2014). Also, this study excluded sites that burned more than twice, because this would complicate attribution of drought intensity according to fire timing. Our finding that drought can impact recovery in single-burn areas may warrant greater attention to drought than fire-return interval for chaparral ecology and management.

We find that landscape-scale variations in recovery among the drought-impacted sites are somewhat predictable ($R^2 = 0.53$) based on terrain, vegetation, soils, and visible reflectance index data (Table 4). The LFM-sensitive VARI derived from Landsat imagery is a strong and negative predictor of recovery within the study areas, particularly when normalized for shrub cover variation. This outcome may support the interpretation that resprouting chaparral in mesic locations is most subject to drought-fire impact. Notably, Peterson and others (2008) showed that differences between chaparral landscapes reduce the spatial correlation of VARI to LFM ($R^2 = 0.59$), as compared to within-site serial correlation through a season ($R^2 = 0.78$). Our use of single prefire Landsat images may yield different VARI patterns than would images from other years or seasons, but we deemed the early-June observations from a non-drought year (1986) to be representative of LFM under high-growth conditions. With clearer understanding of the LFM-drought effect relationship (and additional predictor variables), the regression model herein could be adapted to prioritize locations for ecological study or conservation along xeric chaparral ecotones.

The vast majority (58–69%) of variation in postfire recovery is unexplained by seasonal drought metrics and other geospatial variables evaluated in this study. Part of this uncertainty is attributable to the Landsat-based dFSC data, part may stem from spatial misalignments and scale differences among the data sets, and part is likely due to a lack of data on potentially significant yet unquantified variables. Monthly drought indices aggregated into seasonal periods do not capture important meteorological variations that occur on diurnal or weekly time-scales. The CWD index incorporates data on soil properties and meteorological estimations that are not fully reliable (Flint and others 2013). Application of localized calibration plots was effective in normalizing spatial biases in the NDVI-FSC relation due to aridity and plant community type differences across the region. However, Landsat NDVI-based metrics of FSC exhibited R^2 values of 0.56–0.95 in this study, and thus entail uncertainty when sampled in a spatially explicit manner. Cross-comparison of dFSC to other data sets of differing spatial resolutions and positional accuracies can also cause error in spatial analysis (Foody 2007). Additionally, NDVI trajectories that are more temporally resolved (*e.g.*, intra-seasonally) are required to better elucidate the chronological aspect of drought impact on recovering chaparral. Our analysis of landscape-scale patterns of recovery (Figure 6) suggests that detailed maps of plant species may enable a more substantive

analysis than was feasible using maps of plant community types. Finally, it was beyond the scope of this study to evaluate the 2012–2016 drought—which may have impacted chaparral stands that were completely or mostly recovered from prior fires by 2012—due to the limited time-frames of the CWD and PRCP data. Our finding that drought in seasons close to fire events is most impactful on recovery suggests that—although the 2012–2016 drought may have led to shrub mortalities—such impacts are most likely not due to interruption of postfire recovery in our study areas. Our Landsat NDVI trajectory data suggest that annual shrub growth declined in 2014–2016 but rebounded to normal levels in 2017–2018, and was not outside the historical range of variability in 2012–2018.

Despite the uncertainties noted above, this study is a contribution to the ecology of disturbance in southern Californian chaparral. It provides empirical evidence consistent with the following hypothesis: the locations of fires relative to climatic gradients—and stochastic timing of fire relative to drought intensity fluctuation—conjointly influence patterns of recovery, which determine long-term structural and compositional stability of chaparral. This study should raise further questions tractable by remote sensing, field work, modeling, or laboratory experiment. Analyses that are temporally resolved at intra-seasonal scales and supported by spatially explicit plant species data are needed to better explain drought-fire sensitivity in chaparral. Seasonal Landsat NDVI trajectories during early postfire recovery and between sequential fire events may show critical thresholds with respect to drought intensity, and clarify the relationship of drought to short-interval fire impact. Evaluation of large-scale patterns in vegetation change based on time-sequential remote sensing will continue to be important in future decades, as disturbance regimes and plant communities continue to evolve.

FUNDING

REFERENCES

Abatzoglou JT, McEvoy DJ, Redmond KT. 2017 The West Wide Drought Tracker: drought monitoring at fine spatial scales. Bull Am Meteorol Soc 98(9):1815–20.

Baldocchi D, Falge E, Gu L, Olson R, Hollinger D, Running S, Fuentes J. 2001 FLUXNET: a new tool to study the temporal and spatial variability of ecosystem-scale carbon dioxide, water vapor, and energy flux densities. Bull Am Meteorol Soc 82(11):2415–34.

Batllori E, De Cáceres M, Brotons L, Ackerly DD, Moritz MA, Lloret F. 2019 Compound fire-drought regimes promote ecosystem transitions in Mediterranean ecosystems. J Ecol 107(3):1187–98.

Cayan DR, Redmond KT, Riddle LG. 1999 ENSO and hydrologic extremes in the western United States. J Clim 12(9):2881–93.

Christensen NL, Muller CH. 1975 Effects of fire on factors controlling plant growth in Adenostoma chaparral. Ecol Monogr 45(1):29–55.

Crausbay SD, Ramirez AR, Carter SL, Cross MS, Hall KR, Bathke DJ, Dunham JB. 2017 Defining ecological drought for the twenty-first century. Bull Am Meteorol Soc 98(12):2543–50.

Coates A Dennison P, Roberts D, Roth K. 2015 Monitoring the impacts of severe drought on southern California chaparral species using hyperspectral and thermal infrared imagery. Remote Sens 7(11):14276–91.

Costanza R, d'Arge R, De Groot R, Farber S, Grasso M, Hannon B, Limburg K, Naeem S, O'Neill RV, Paruelo J, Raskin RG. 1997 The value of the world's ecosystem services and natural capital. Nature 387(6630):253–60.

Daly C, Neilson RP, Phillips DL. 1994 A statistical-topographic model for mapping climatological precipitation over mountainous terrain. J Appl Meteorol 33(2):140–58.

Davis FW, Goetz S. 1990 Modeling vegetation pattern using digital terrain data. Landscape Ecol 4(1):69–80.

Davis SD, Ewers FW, Sperry JS, Portwood KA, Crocker MC, Adams GC. 2002 Shoot dieback during prolonged drought in Ceanothus (*Rhamnaceae*) chaparral of California: a possible case of hydraulic failure. Am J Bot 89(5):820–8. [PubMed: 21665682]

Davis SD, Pratt RB, Ewers FW, Jacobsen AL. 2007 Freezing tolerance impacts chaparral species distribution in the Santa Monica Mountains Knapp DA, editor. Flora and Ecology of the Santa Monica Mountains. Fullerton (CA): Southern California Botanists, pp 159–72. ISBN 978–0-9796277–0-5.

Díaz-Delgado R, Lloret F, Pons X, Terradas J. 2002 Satellite evidence of decreasing resilience in Mediterranean plant communities after recurrent wildfires. Ecology 83:2293–303.

Díaz-Delgado R, Pons X. 2001 Spatial patterns of forest fires in Catalonia (NE of Spain) along the period 1975–1995: analysis of vegetation recovery after fire. For Ecol Manag 147:67–74. 10.1016/S0378-1127(00)00434-5.

Diffenbaugh NS, Swain DL, Touma D. 2015 Anthropogenic warming has increased drought risk in California. Proc Natl Acad Sci 112(13):3931–6. [PubMed: 25733875]

Fernandez-Manso A, Quintano C, Roberts DA. 2016 Burn severity influence on post-fire vegetation cover resilience from Landsat MESMA fraction images time series in Mediterranean forest ecosystems. Remote Sens Environ 184:112–23. 10.1016/j.rse.2016.06.015.

Flint LE, Flint AL, Thorne JH. 2013 Fine-scale hydrologic modeling for regional landscape applications: the California Basin Characterization Model development and performance. Ecol Process 2(25):1–21.

Foody GM. 2007 Map comparison in GIS. Prog Phys Geogr 31(4):439–45.

Fraser RH, Olthof I, Carrière M, Deschamps A, Pouliot D. 2011 Detecting long-term changes to vegetation in northern Canada using the Landsat satellite image archive. Environ Res Lett 6(4):045502.

Frazer JM, Davis SD. 1988 Differential survival of chaparral seedlings during the first summer drought after wildfire. Oecologia 76(2):215–21. [PubMed: 28312199]

Gitelson AA, Stark R, Grits U, Rundquist D, Kaufman Y, Derry D. 2002 Vegetation and soil lines in visible spectral space: a concept and technique for remote estimation of vegetation fraction. Int J Remote Sens 23(13):2537–62.

Griffin D, Anchukaitis KJ. 2014 How unusual is the 2012–2014 California drought? Geophys Res Lett 41(24):9017–23.

Gouveia C, DaCamara CC, Trigo RM. 2010 Post-fire vegetation recovery in Portugal based on spot/vegetation data. Nat Hazards Earth Syst Sci 10:673–84. 10.5194/nhess-10-673-2010.

Harvey RA, Mooney HA. 1964 Extended dormancy of chaparral shrubs during severe drought. Madroño 17(5):161–3.

Hope A, Tague C, Clark R. 2007 Characterizing post-fire vegetation recovery of California chaparral using TM/ETM + time-series data. Int J Remote Sens 28(6):1339–54.

Jacobsen AL, Davis SD, Fabritius SL. 2004 Fire frequency impacts non-sprouting chaparral shrubs in the Santa Monica Mountains of southern California In: Arianoutsou M, Papanastasis VP, Eds. Ecology, conservation and management of Mediterranean climate ecosystems. Rotterdam: Millpress p 1–5.

Jacobsen AL, Pratt RB. 2018 Extensive drought-assodated plant mortality as an agent of type-conversion in chaparral shrublands. New Phytol 219(2):498–504. [PubMed: 29727471]

Jacobsen AL, Tobin MF, Toschi HS, Percolla MI, Pratt RB. 2016 Structural determinants of increased susceptibility to dehydration-induced cavitation in post-fire resprouting chaparral shrubs. Plant Cell Environ 39(11):2473–85. [PubMed: 27423060]

Keeley JE, Brennan TJ. 2012 Fire-driven alien invasion in a fire-adapted ecosystem. Oecologia 169 (4): 1043–52. [PubMed: 22286083]

Keeley JE, Soderstrom TJ. 1986 Postfire recovery of chaparral along an elevational gradient in southern California. Southwestern Nat 31(2): 177–84.

Key CH, Benson NC. 1999 The Normalized Bum Ratio (NBR): A Landsat TM radiometric measure of burn severity United States Geological Survey, Northern Rocky Mountain Science Center Bozeman (MT).

Kolb KJ, Davis SD. 1994 Drought tolerance and xylem embolism in co-occurring species of coastal sage and chaparral. Ecology 75(3):648–59.

Lanorte A, Lasaponara R, Lovallo M, Telesca L. 2014 Fisher-Shannon information plane analysis of SPOT/VEGETATION Normalized Difference Vegetation Index (NDVI) time series to characterize vegetation recovery after fire disturbance. Int J Appl Earth Observ Geoinf 26:441–6. 10.1016/j.jag.2013.05.008.

Lippitt CL, Stow DA, O'Leary JF, Franklin J. 2013 Influence of short-interval fire occurrence on post-fire recovery of fire-prone shrublands in California, USA. Int J Wildland Fire 22(2):184–93.

Livneh B, Rosenberg EA, Lin C, Nijssen B, Mishra V, Andreadis KM, Lettenmaier DP. 2013 A long-term hydrologically based dataset of land surface fluxes and states for the conterminous United States: update and extensions. J Clim 26(23):9384–92.

MacDonald GM. 2007 Severe and sustained drought in southern California and the West: Present conditions and insights from the past on causes and impacts. Q Int 173:87–100.

Mao Y, Nijssen B, Lettenmaier DP. 2015 Is climate change implicated in the 2013–2014 California drought? A hydrologic perspective. Geophys Res Lett 42(8):2805–l 3.

Masek JG, Vermote EF, Saleous NE, Wolfe R, Hall FG, Huemmrich KF, Lim TK. 2006 A Landsat surface reflectance dataset for North America 1990–2000. IEEE Geosci Remote Sens Lett 3(1):68–72.

Matyas WJ, Parker I. 1980 CALVE G mosaic of existing vegetation of California. US Forest Service: Regional Ecology Group.

McCullough IM, Davis FW, Dingman JR, Flint LE, Flint AL, Serra-Diaz JM, Franklin J. 2016 High and dry: high elevations disproportionately exposed to regional climate change in Mediterranean-climate landscapes. Landscape Ecol 31(5):1063–75.

McDowell N, Pockman WT, Allen CD, Breshears DD, Cobb N, Kolb T, Yepez EA. 2008 Mechanisms of plant survival and mortality during drought: why do some plants survive while others succumb to drought? New Phytol 178(4):719–39. [PubMed: 18422905]

McMichael CE, Hope AS, Roberts DA, Anaya MR. 2004 Post-fire recovery of leaf area index in California chaparral: a remote sensing-chronosequence approach. Int J Remote Sens 25(21):4743–60.

Meentemeyer RK, Moody A. 2002 Distribution of plant life history types in California chaparral: the role of topographically-determined drought severity. J Veg Sci 13(1):67–78.

Meng R, Dennison P, D'Antonio C, Moritz M. 2014 Remote sensing analysis of vegetation recovery following short-interval fires in southern California Shrublands. PloS One 9(10):e110637. [PubMed: 25337785]

Miller JD, Thode AE. 2007 Quantifying burn severity in a heterogeneous landscape with a relative version of the delta Normalized Bum Ratio (dNBR). Remote Sens Environ 109(1):66–80.

Mills JN. 1983 Herbivory and seedling establishment in post-fire southern California chaparral. Oecologia 60(2):267–70. [PubMed: 28310496]

Minchella A, Del Frate F, Capogna F, Anselmi S, Manes F. 2009 Use of multitemporal SAR data for monitoring vegetation recovery of Mediterranean burned areas. Remote Sens Environ 113:588–97. 10.1016/j.rse.2008.11.004.

Moreno JM, Oechel WC. 1993 Demography of Adenostoma fasciculatum after fires of different intensities in southern California chaparral. Oecologia 96(1):95–101. [PubMed: 28313758]

Oechel WC, Lawrence W. 1981 Carbon allocation and utilization In: Miller PC, Ed. Resource use by chaparral and matorral. New York: Springer, p 185–235.

Paddock WA, Davis SD, Pratt RB, Jacobsen AL, Tobin MF, López-Portillo J, Ewers FW. 2013 Factors determining mortality of adult chaparral shrubs in an extreme drought year in California. Aliso J Syst Evol Bot 31(1):49–57.

Palmer WC. 1965 Meteorological drought. Research Paper 45, U.S. Department of Commerce, 58 pp.

Parsons DJ, Rundel PW, Hedlund RP, Baker GA. 1981 Survival of severe drought by a non-sprouting chaparral shrub. Am J Bot 68(7):973–9.

Pausas JG, Pratt RB, Keeley JE, Jacobsen AL, Ramirez AR, Vilagrosa A, Davis SD. 2016 Towards understanding resprouting at the global scale. New Phytol 209(3):945–54. [PubMed: 26443127]

Peterson SH, Roberts DA, Dennison PE. 2008 Mapping live fuel moisture with MODIS data: a multiple regression approach. Remote Sens Environ 112(12):4272–84.

Petropoulos GP, Griffiths HM, Kalivas DP. 2014 Quantifying spatial and temporal vegetation recovery dynamics following a wildfire event in a Mediterranean landscape using EO data and GIS. Appl Geogr 50:120–31. 10.1016/j.apgeog.2014.02.006.

Pratt RB, Jacobsen AL, Ramirez AR, Helms AM, Traugh CA, Tobin MF, Davis SD. 2014 Mortality of resprouting chaparral shrubs after a fire and during a record drought: physiological mechanisms and demographic consequences. Glob Change Biol 20(3):893–907.

Radosevich SR, Conard SG. 1980 Physiological control of chamise shoot growth after fire. Am J Bot 67(10):1442–7.

Riaño D, Chuvieco E, Ustin S, Zomer R, Dennison P, Roberts D, Salas J. 2002 Assessment of vegetation regeneration after fire through multitemporal analysis of AVIRIS images in the Santa Monica Mountains. Remote Sens Environ 79:60–71.

Roberts DA, Dennison PE, Peterson S, Sweeney S, Rechel J. 2006 Evaluation of Airborne Visible/ Infrared Imaging Spectrometer (AVIRIS) and Moderate Resolution Imaging Spectrometer (MODIS) measures of live fuel moisture and fuel condition in a shrubland ecosystem in southern California. J Geophys Res : Biogeosci 111(G4):1–16.

Röder A, Hill J, Duguy B, Alloza JA, Vallejo R. 2008 Using long time series of Landsat data to monitor fire events and post-fire dynamics and identify driving factors: a case study in the Ayora region (eastern Spain). Remote Sens Environ 112(1):259–73.

Seager R, Hooks A, Williams AP, Cook B, Nakamura J, Henderson N. 2015 Climatology, variability, and trends in the US vapor pressure deficit, an important fire-related meteorological quantity. J Appl Meteorol Climatol 54(6):1121–41.

Serra-Diaz JM, Franklin J, Sweet LC, McCullough IM, Syphard AD, Regan HM, Redmond K. 2016 Averaged 30 year climate change projections mask opportunities for species establishment. Ecography 39(9):844–5. 10.1111/ecog.02074.

Shoshany M 2000 Satellite remote sensing of natural Mediterranean vegetation: a review within an ecological context. Prog Phys Geogr 24(2):153–78.

Smith AG, Newingham BA, Hudak AT, Bright BC. 2019 Got shrubs? Precipitation mediates long-term shrub and introduced grass dynamics in chaparral communities after fire. Fire Ecol 15(12):1–16. 10.1186/s42408-019-0031-2.

Solans Vila JP, Barbosa P. 2010 Post-fire vegetation regrowth detection in the Deiva Marina region (Liguria-Italy) using Landsat TM and ETM + data. Ecol Model 221:75–84. 10.1016/j.ecolmodel.2009.03.011.

Stephenson N 1998 Actual evapotranspiration and deficit: biologically meaningful correlates of vegetation distribution across spatial scales. J Biogeogr 25(5):855–70.

Storey EA, Stow DA, O'Leary JF. 2016 Assessing postfire recovery of chamise chaparral using multi-temporal spectral vegetation index trajectories derived from Landsat Imagery. Remote Sens Environ 183:53–64.

Stow D, Niphadkar M, Kaiser J. 2005 MODIS-derived visible atmospherically resistant index for monitoring chaparral moisture content. Int J Remote Sens 26(17):3867–73.

Syphard AD, Brennan TJ, Keeley JE. 2019a Drivers of chaparral type conversion to herbaceous vegetation in coastal Southern California. Diver Distrib 25(1):90–101.

Syphard AD, Brennan TJ, Keeley JE. 2019b Extent and drivers of vegetation type conversion in Southern California chaparral. Ecosphere 10(7):e02796.

Syphard AD, Keeley JE. 2017 Historical reconstructions of California wildfires vary by data source. Int Wildland Fire 25(12):1221–7.

Szép IJ, Mika J, Dunkel Z. 2005 Palmer drought severity index as soil moisture indicator: physical interpretation, statistical behaviour and relation to global climate. Phys Chem Earth Parts A/B/C 30(1–3):231–43.

Turner MG. 2010 Disturbance and landscape dynamics in a changing world. Ecology 91 (10):2833–49. [PubMed: 21058545]

Venturas MD, MacKinnon ED, Dario HL, Jacobsen AL, Pratt RB, Davis SD. 2016 Chaparral shrub hydraulic traits, size, and life history types relate to species mortality during California's historic drought of 2014. PloS One 11(7):e0159145. [PubMed: 27391489]

Vermote E, Justice C, Claverie M, Franch B. 2016 Preliminary analysis of the performance of the Landsat 8/OLI land surface reflectance product. Remote Sens Environ 185:46–56. [PubMed: 32020955]

Viedma O, Meliá J, Segarra D, García-Haro J. 1997 modeling rates of ecosystem recovery after fires by using Landsat TM data. Remote Sens Environ 61:383–98. 10.1016/s0034-4257(97)00048-5.

Vicente-Serrano SM, Pérez-Cabello F, Lasanta T. 2011 Pinus halepensis regeneration after a wildfire in a semiarid environment: assessment using multitemporal Landsat images. Int J Wildland Fire 20:195–208. 10.1071/wf08203.

Vitousek PM, Mooney HA, Lubchenco J, Melillo JM. 1997 Human domination of Earth's ecosystems. Science 277(5325):494–9.

Wittenberg L, Malkinson D, Beeri O, Halutzy A, Tesler N. 2007 Spatial and temporal patterns of vegetation recovery following sequences of forest fires in a Mediterranean landscape. Mt. Carmel Israel. Catena 71:76–83. 10.1016/j.catena.2006.10.007.

Westerling AL, Hidalgo HG, Cayan DR, Swetnam TW. 2006 Warming and earlier spring increase western US forest wildfire activity. Science 313(5789):940–3. [PubMed: 16825536]

Williams AP, Allen CD, Macalady AK, Griffin D, Woodhouse CA, Meko DM, Dean JS. 2013 Temperature as a potent driver of regional forest drought stress and tree mortality. Nat Clim Change 3(3):292–7.

Yoon JH, Wang SS, Gillies RR, Kravitz B, Hipps L, Rasch PJ. 2015 Increasing water cycle extremes in California and in relation to ENSO cycle under global warming. Nat Commun 6(8657):1–6.

Zedler PH, Gautier CR, McMaster GS. 1983 Vegetation change in response to extreme events: the effect of a short interval between fires in California chaparral and coastal scrub. Ecology 64(4):809–18.

Zhu Z, Woodcock E. 2012 Object-based cloud and cloud shadow detection in Landsat imagery. Remote Sens Environ 118:83–94.

Highlights

- Postfire recovery of chaparral was evaluated across southern California (1984–2018).

- Drought in wet seasons surrounding fire events significantly affected recovery.

- Geographic range of chaparral may be contracting due to drought-fire in xeric areas.
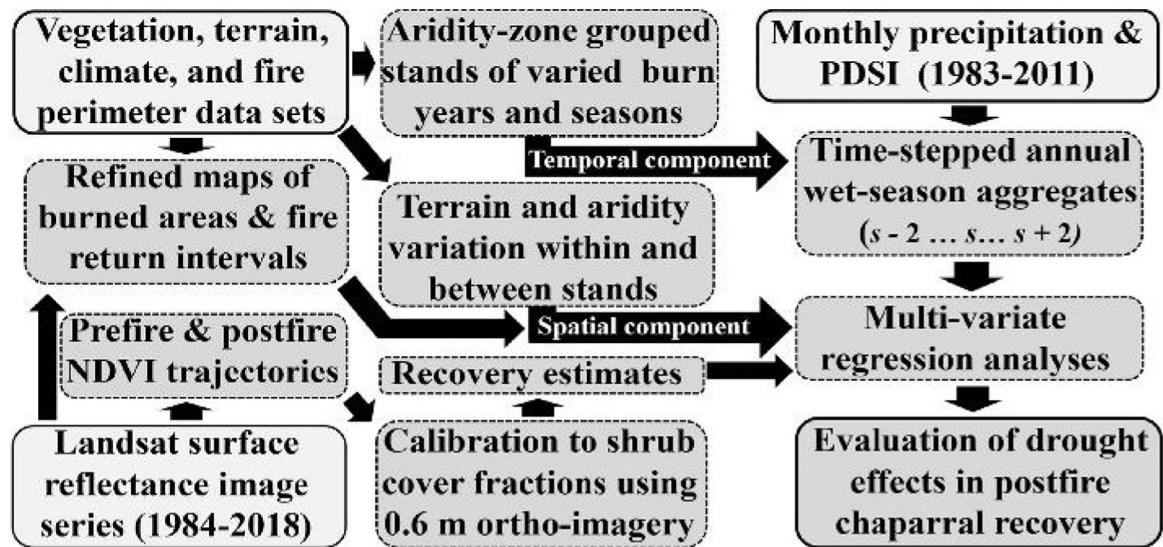
Figure 1.
Flowchart depicting how key data sets are used in order to address the spatial and temporal components of drought impact upon postfire chaparral recovery. Lighter shaded boxes represent source data, while darker ones indicate data processing and analytical steps.
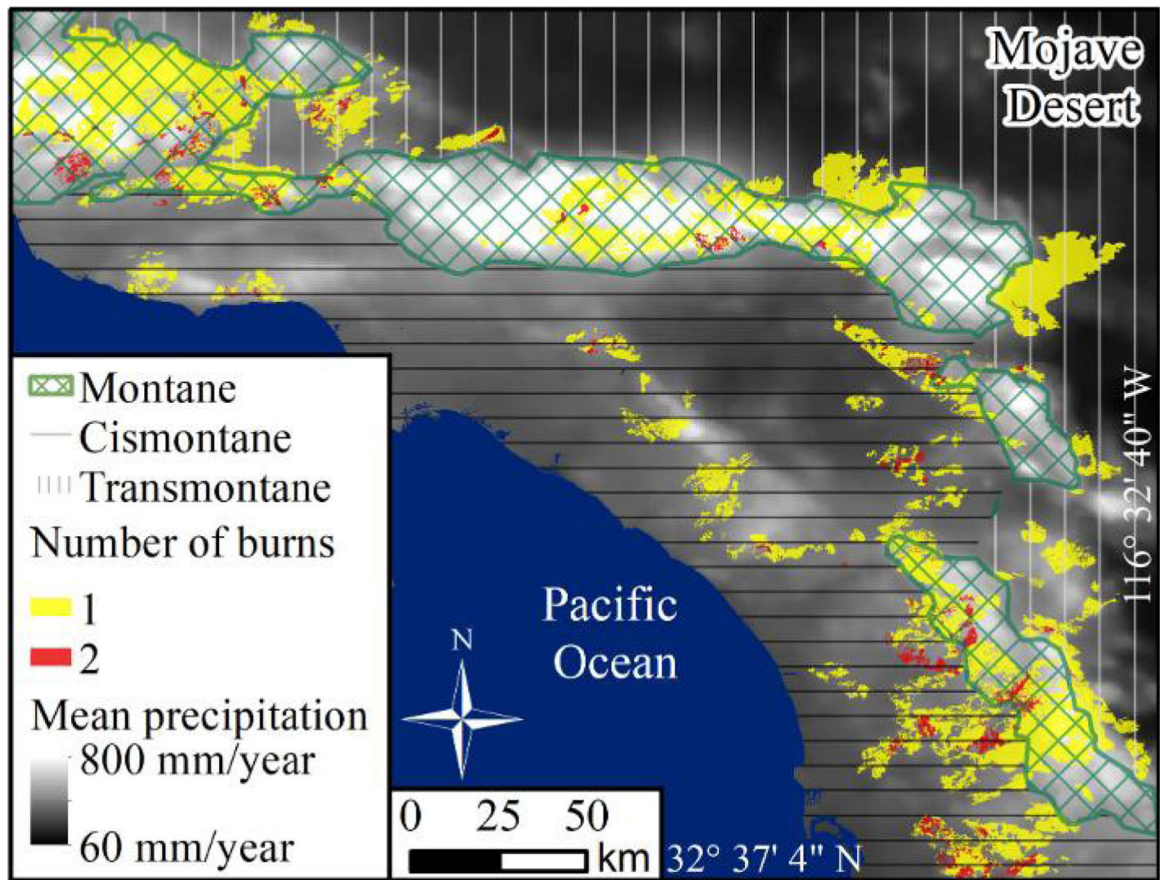
Figure 2.
Map of burned chaparral stands included in this study, displayed per number of burns in the period 1985–2008. Montane zone boundaries coincide with 500 mm mean annual precipitation contours, which are based on a 30-year gridded climate normal (prism.oregonstate.edu) displayed by a min-max contrast stretch (values exceed 800 mm per year in some locations).
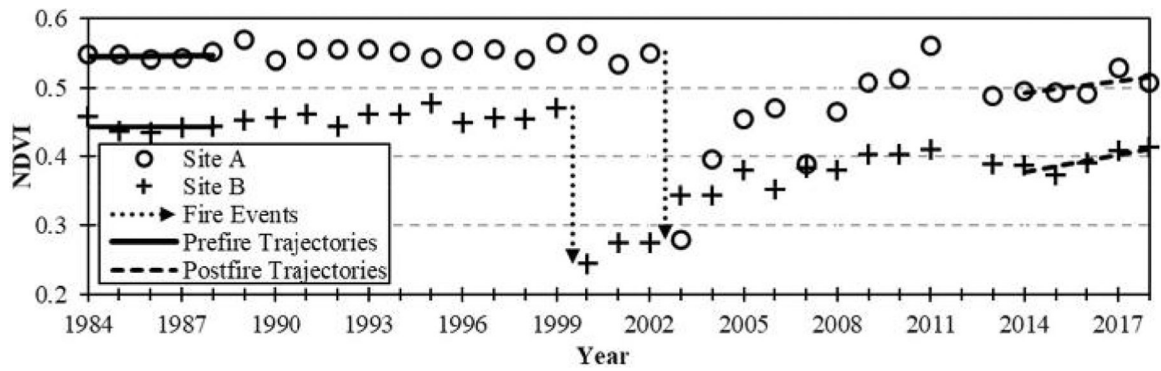
Figure 3.
Examples of Normalized Difference Vegetation Index (NDVI) series based on pixels from two exemplary burned sites (A and B) in eastern San Diego County. Metrics applied to the prefire 1984–1988 (5-year means) and postfire (2014–2018) periods (linear best-fit functions) are shown along with fire event timings at each site. The NDVI series represented in this figure were normalized for phenological artifacts using unburned control sites.

Figure 4.
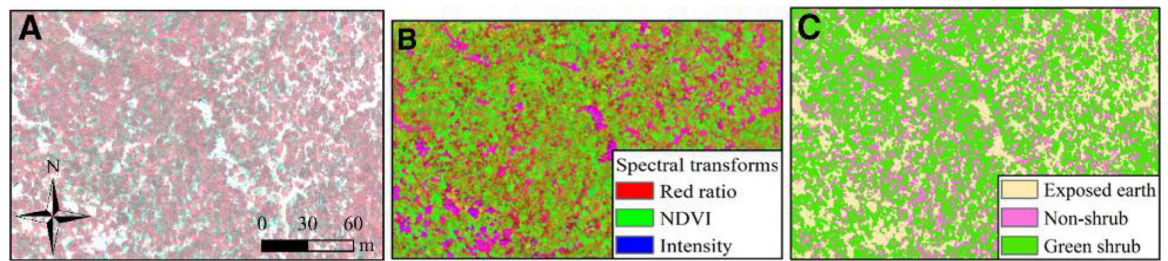Illustration of fine-scale aerial ortho-image data used to derive empirical relations between fractional shrub cover and Landsat NDVI. **A** color-infrared ortho-image of 0.6-m spatial resolution displayed in true color, **B** false-color composite of spectral transformations used in classification, and **C** decision-tree classification used to distinguish green shrub cover from exposed earth and non-shrub vegetation.
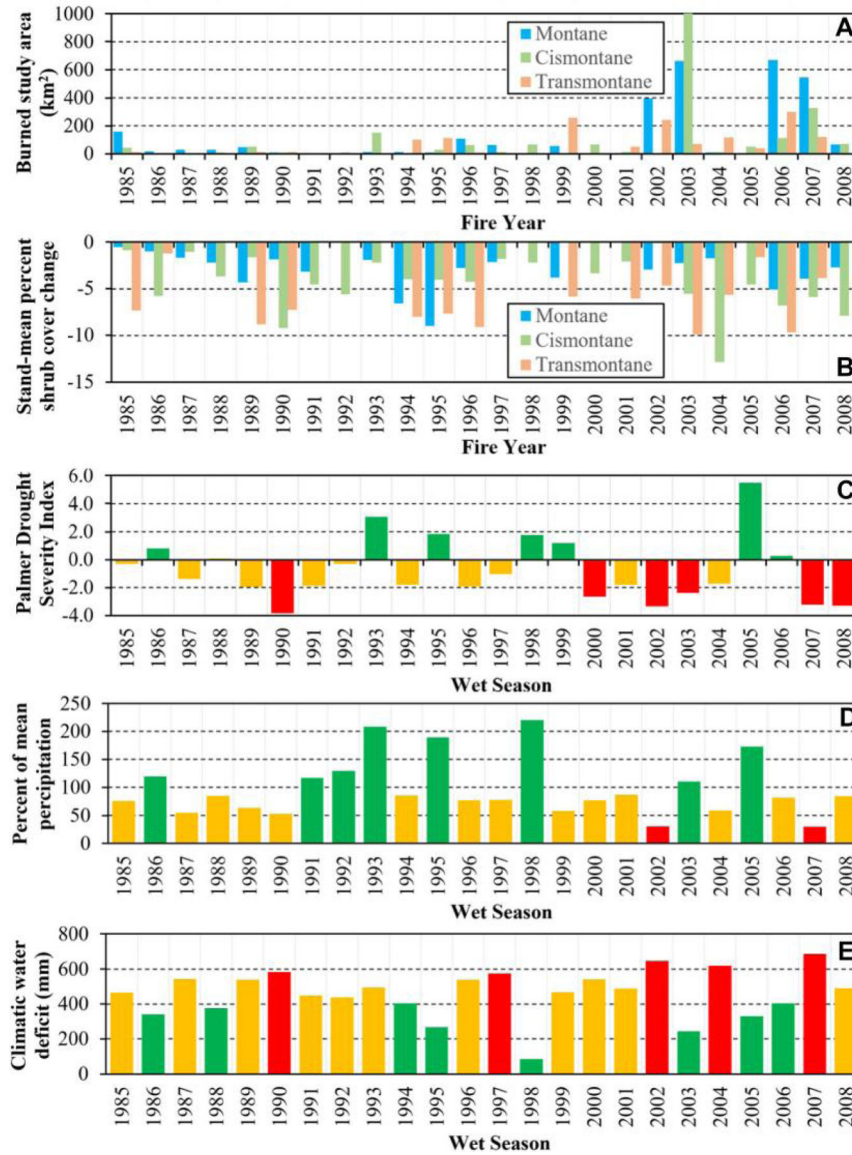
Figure 5.

A Areal coverage of single-bum study areas within the montane, cismontane, and transmontane zones of southern California chaparral; **B** mean percent shrub cover change in stands aggregated by burn year; average wet-season (Nov. of prior year to May of labeled year) drought-metric values within the stands, including **C** Palmer Drought Severity Index (PSDI), **D** percent of the mean precipitation of the period 1983–2011, and **E** climatic water deficit. Green bars denote non-drought, orange bars denote moderate drought, and red bars suggest extreme drought based on each metric. Drought severity based on PDSI values in years of the time series not represented here includes 1983 (5.3), 1984 (– 0.1), 2009 (– 3.6), 2010 (0.3), and 2011 (2.85).

Figure 6.

Spatial patterns of postfire recovery (based on Landsat NDVI trajectories) within selected, drought-impacted stands. Frame *f* indicates loc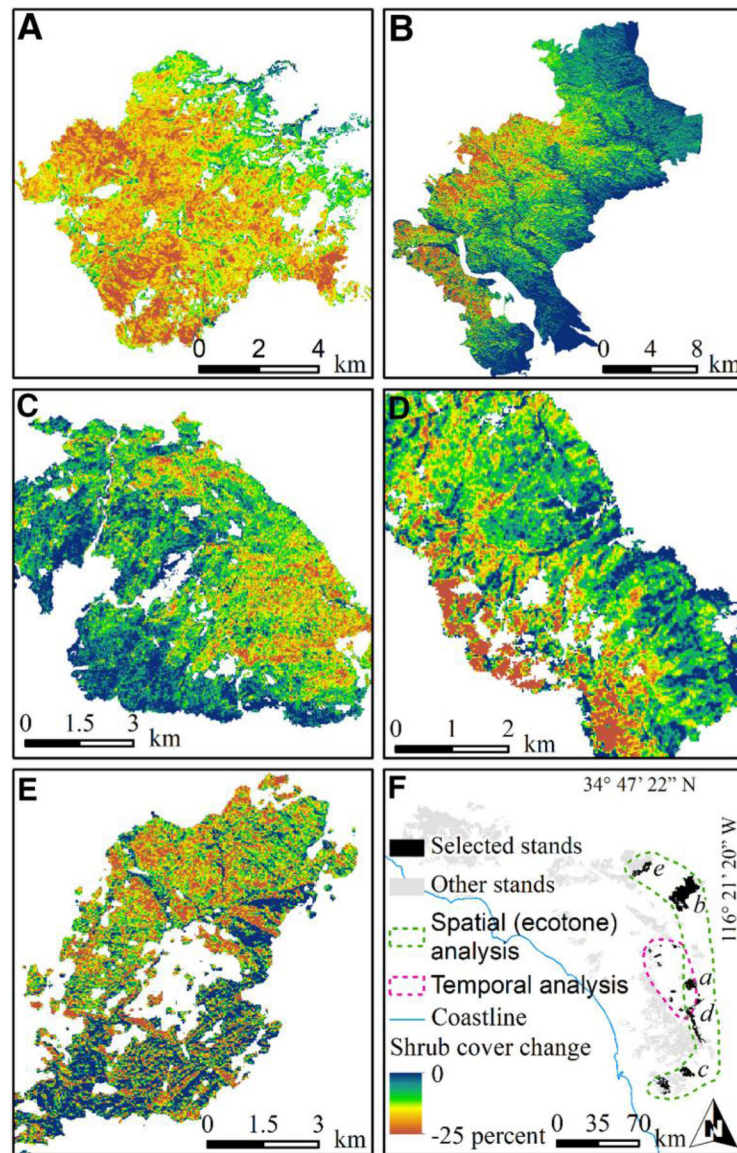ations of all study areas relative to selected drought-impacted stands: transmontane xeric sites include **A**, **B**, and **D**; site **A** is cismontane; site *e* is high-elevation montane. Half of the stands used in temporal analysis (**F**) were well recovered.

Table 1.

Geospatial Data Sets Used to Explain Postfire Chaparral Recovery

Data set	Variable(s)	Data origin site	Spatial resolution	Temporal properties
CALVEG	Plant community type	fs.usda.gov	1.6–3.2 km	Produced in 1977–1979
FVEG	Plant community type	fs.usda.gov	250 m	Revised in 2015
State Soil Geographic	Hydrologically relevant soil characteristics (7)	nrcs.usda.gov	1 km	Produced in 1997
30-year mean annual climate	Precipitation, temperature, vapor pressure deficit	prism.oregonstate.edu	800 m	Based upon monthly means (1981–2011)
Terrain	Elevation, slope, aspect, curvature, surface irradiance	ned.usgs.gov	30 m	–
Riparian zones	30-m proximity to streams	data.cnra.ca.gov	30 m	–
Visible Atmospherically Resistant Index	Sensitive to live-fuel moisture, derived from Landsat 5 images	espa.cr.usgs.gov	30 m	Single observations from 13 June 1986
Monthly precipitation	Precipitation used in the Livneh and others (2013) model	data.nodc.noaa.gov	6 km	Monthly estimates from 1983 to 2011 included
Palmer Drought Severity Index	Water deficit based on soils, temperature, precipitation	wrcc.dri.edu	4 km	Monthly estimates from 1983 to 2011
Climatic water deficit	Total evaporative demand relative to soil moisture	Climate.calcommons.org	270 m	Monthly estimates from 1983 to 2010

NASA Author Manuscript NASA Author Manuscript NASA Author Manuscript NASA Author Manuscript

Table 2.

Results of Least-Squares Linear Regressions

Climate zone	Variable	p	t	β Coef.	Fraction of explained variance	Slope (α)	SE	Collinearity tolerance	VIF	Model Adj. R^2
Montane	Wet-season PRCP-S_{-2}	0.03*	−2.25	−0.16	0.14	−1.20	0.53	0.60	1.66	0.26
	Summer PDSI-S_{+2}	0.01*	2.51	0.20	0.26	0.01	0.00	0.49	2.02	**0.27**
Cismontane	Wet-season PRCP-S_0	0.04*	2.04	0.18	0.20	3.81	1.87	0.73	1.36	0.10
	Summer CWD-S_{-0}	0.04*	2.04	0.23	0.26	0.30	0.15	0.43	2.32	0.15
	Wet-season CWD-S_{-1}	0.00**	3.00	0.32	0.23	0.17	0.06	0.48	2.09	**0.16**
	Wet-season CWD-S_{-2}	0.02*	2.42	0.28	0.20	0.13	0.05	0.41	2.44	
Transmontane	Wet-season PRCP-S_{-1}	0.00**	−3.60	−0.42	0.30	−7.02	1.95	0.48	2.09	0.35
	Wet-season PRCP-S_{+1}	0.03*	2.20	0.25	0.18	3.53	1.60	0.51	1.96	
	Summer PDSI-S_{-2}	0.05*	2.00	0.27	0.14	0.01	0.00	0.33	3.06	0.39
	Summer PDSI-S_{-1}	0.00***	−3.89	−0.35	0.18	−0.01	0.00	0.75	1.34	
	Summer PDSI-S_{+1}	0.01**	2.86	0.33	0.18	0.01	0.00	0.45	2.25	
	Summer PDSI-S_{+2}	0.04*	2.11	0.26	0.14	0.01	0.00	0.41	2.47	
	Summer CWD-S_{-2}	0.05*	1.98	0.24	0.27	0.14	0.07	0.45	2.25	0.35
	Wet-season CWD-S_{-1}	0.00**	4.55	0.56	0.34	0.24	0.05	0.39	2.58	**0.41**
	Wet-season CWD-S_{+1}	0.01**	−2.84	−0.34	0.21	−0.17	0.06	0.40	2.50	

These were used to evaluate seasonal precipitation (PRCP), climatic water deficit (CWD), and Palmer Drought Severity Index (PDSI) drought metrics as explanatory variables of postfire recovery (dFSC). Only significant metrics and seasons are shown. Mean annual precipitation and temperature are also significant in each test but were excluded from this table. In bold font are Adjusted R^2 values that are highest for each climate zone, including montane (n = 223), cismontane (n = 161), and transmontane (n = 107).

*
p < 0.050;

**
p < 0.010;

***
p < 0.001.

Table 3.

Results of Landscape-Scale Regression Tests

Variable	p	t	β Coef.	Slope (α)	SE	Collinearity tolerance	VIF	Model Adj. R^2
Difference in wet-season PRCP-S_{-2}	0.01 **	2.62	0.22	2.33	0.89	0.64	1.58	0.05
Difference in wet-season PRCP-S_{+1}	0.04 *	2.05	0.20	1.78	0.87	0.49	2.06	
Summer PDSI-S_{-1}	0.04 *	2.02	0.12	0.00	0.00	0.69	1.44	0.06
Summer PDSI-S_0	0.00 **	3.02	0.15	0.00	0.00	0.89	1.12	
Summer PDSI-S_{+2}	0.00 ***	3.74	0.18	0.00	0.00	0.96	1.04	
Difference in summer PDSI-S_{-2}	0.00 ***	4.05	0.32	0.00	0.00	0.73	1.38	0.07
Summer CWD-S_{-2}	0.00 **	3.29	0.23	0.13	0.04	0.44	2.29	0.09
Wet-season CWD-S_{+2}	0.00 ***	− 3.54	− 0.19	− 0.06	0.02	0.78	1.28	0.05

These were used to evaluate differences in recovery (n = 208) between 416 paired single and multiple-burn sites, as a function of fire-return interval and drought metrics based on wet and summer season precipitation (PRCP), Palmer Drought Severity Index (PDSI), and climatic water deficit (CWD).

*
p < 0.050;

**
p < 0.010;

***
p < 0.001.

Table 4.

Results from Landscape-Scale Spatial Analysis

Variable	p	t	β Coef.	Slope (a)	Standard Error	Collinearity tolerance	VIF
Elevation	<0.001	−6.00	−0.35	−0.01	0.00	0.60	1.66
Plant community	<0.001	10.27	0.12	2.01	0.70	0.78	1.29
Soil Permeability	<0.001	−7.85	0.14	−0.45	0.26	0.48	2.09
Visible Atmospherically Resistant Index	<0.001	18.45	−0.38	31.87	1.73	0.88	1.14

An ordinary least-squares regression test used to significant explanatory variables of postfire recovery samples (n = 697) at ten drought-impacted chaparral stands in southern California. Adj. $R^2 = 0.53$; SE = 2.58; df[= 4; Fsig < 0.001.

Table 5.

Regional Analysis of Drought Impact on Recovery

Variable	p	t	β Coef.	Slope (α)	SB	Collinearity tolerance	VIF	Individual R^2	Fraction of variance explained
Mean CWD	0.000	4.75	0.89	1.10	0.23	0.22	4.55	0.06	0.24
CWD-S_{-3}	0.002	-3.24	-0.96	-1.01	0.31	0.09	11.31	0.00	0.26
CWD-S_{-2}	0.001	-3.52	-1.17	-0.44	0.12	0.07	14.15	0.04	0.31
CWD-S_{-1}	0.111	-1.62	-0.51	-0.21	0.13	0.08	12.56	0.09	0.00
CWD-S_0	0.002	-3.14	-0.73	-0.35	0.11	0.14	6.92	0.13	0.19
CWD-S_{+1}	0.192	1.32	0.58	0.38	0.29	0.04	24.90	0.11	0.00
CWD-S_{+2}	0.619	0.50	0.14	0.06	0.11	0.10	9.94	0.00	0.00
CWD-S_{+3}	0.083	1.76	0.95	0.37	0.21	0.03	37.06	0.11	0.00
CWD-S_{+4}	0.25	1.17	1.55	0.44	0.16	0.15	17.50	0.00	0.00
CWD-S_{+5}	0.78	-0.27	-0.41	-0.10	0.33	0.27	14.63	0.00	0.00

Results are from univariate (individual-variable) and multivariate linear regressions used to evaluate postfire recovery (change in fractional shrub cover) relative to climatic water deficit (CWD) in wet-season cycles relative to time-of-fire at twelve stands (sample plot n =75), and long-term (27-year) wet-season mean CWD values. Adj. R^2 = 0.42; Standard Error (SE) = 5.4; df$_1$ = 8; Fsig < 0.001.